J Electr Eng Technol.2018; 13(2): 1008-1020
http://doi.org/10.5370/JEET.2018.13.2.1008

ISSN(Print) 1975-0102
ISSN(Online) 2093-7423

Dynamic Compliance and its Compensation Control of HIVC Force Control System

Kai-xian Ba*, Bin Yu†, Wen-feng Li*, Dong-kun Wang*, Ya-liang Liu*, Guo-liang Ma* and Xiang-dong Kong**

Abstract – In this paper, the dynamic compliance and its compensation control of the force control system on the highly integrated valve-controlled cylinder (HIVC), the joint driver of the hydraulic drive legged robot, is researched. During the robot motion process, the outer loop dynamic compliance control is applied on the base of hydraulic control inner loop and most inner loop control are the force or torque closed loop control. While the dynamic compliance control effectiveness of outer loop can be affected by the inner loop self-dynamic-compliance. Based on this problem, the dynamic compliance series composition theory of HIVC force control system as well as the analysis of its self-dynamic-compliance is proposed. And then the paper comes up with the compliance-enhanced control, which is a compound compensation control method of dynamic compliance with multiple series branches. Finally, the experiment results indicate that the control method mentioned above can enhance the dynamic compliance of HIVC force control system observably. This provides the compensation control method of inner loop dynamic compliance for the outer loop compliance control requiring the high accuracy and high robustness for the robot.

Keywords: Legged robot, Highly integrated valve-controlled cylinder, Force control, Dynamic compliance, Compensation control

1. Introduction

The valve-controlled cylinder is the most common component in the hydraulic system and has a wide range of application in the industry filed, such as the aerospace filed, the metallurgy field, the engineering machinery filed, the agricultural machinery filed and the advanced manufacturing field. Compared with the valve-controlled cylinder, the highly integrated valve-controlled cylinder (HIVC) has a higher power-to-weight ratio. It shows the extraordinary advantages on such mechanism, as the aerospace load simulator, the high performance legged robot and so on. Unlike the traditional civil mechanical equipment, the mechanism above should possess excellent control performance, which can make them obtain better adaptability in the complex environment. Therefore, as the driver of those mechanism, the HIVC should be designed with higher standards. Those standards are involved with the lighter weight, the faster response and many other characteristics. That improves the practical application value of the research on structure design optimization and control compensation method for HIVC [1-4].

† Corresponding Author: School of mechanical engineering, Yanshan University, China. (yb@ysu.edu.cn)
* School of mechanical engineering, Yanshan University, China. (bkx @ysu.edu.cn, xrlzlwf@stumail.ysu.edu.cn, wdk2015@outlook.com, liuyaliang666@163.com, mgl@stumail.ysu.edu.cn)
** Hebei Provincial Key Laboratory of Heavy Machinery Fluid Power Transmission and Control, China. (xdkong@ysu.edu.cn)
Received: August 22, 2016; Accepted: December 8, 2017

The researches on system dynamic compliance control are widespread in the legged robot control domain. It can be learned from those researches that, when the load with large stiffness acts on the robot foot end, the dynamic compliance control is can provide the robot with certain compliance to reduce the rigid impact effectively. That also prevents the robot's mechanical structure from being damaged and brings a better entire motion control performance. While that dynamic compliance can be indicated by the dynamic characteristic of system output when the system is under the effect of external disturbance. Moreover, the impedance control method is taken as the common control method of second order dynamic compliance, which is widely applied in the motor drive legged robot domain, such as Tekken [5], Scout [6], KOLT [7] and so on. That control method can be used by making the system be equivalent to the ideal second order mass-stiffness-damping system with desired stiffness, desired damping and desired mass. In recent years, the hydraulic drive legged robot is becoming the hot spot of robot research, such as Bigdog [8], HyQ [9], Scalf-1[10] and so on. Most drivers for the leg joint of that kind robot are the HIVC and researchers are trying to apply the impedance-based dynamic compliance control method to those drivers.

In order to conduct the dynamic compliance control on these hydraulic drive legged robots through the HIVC, the HIVC hydraulic control system should be adopted as the inner loop control. Based on that, the outer loop dynamic compliance control is introduced to the system. Therefore,

when the external disturbance acts on the system, the input signal is changed through the outer loop. Then the system can obtain certain dynamic compliance. Besides, within the dynamic compliance control methods of the most references mentioned above, the inner loop force control system is often regarded as the ideal system. So the selection of the control method and the proposal of corresponding compensation control strategy are aimed at the dynamic compliance control outer loop. Yet the entire accuracy of that dynamic compliance is not only determined by the outer loop impedance control but also affected by the accuracy of inner loop control. The basic inner loop control methods of HIVC include the position control and the force control, both of which have great application value. However, precise kinematic planning of contacts is not a feasible solution for robots that have to move and interact in challenging and complex environment. Compared with the position control system, the force control system has faster response speed [11]. Thus the research in this paper is focused on the inner loop force control. Ideally, when the HIVC force closed loop control is adopted as the inner loop control, the self-dynamic-compliance of HIVC force control system tends to be infinite. In other words, the force control accuracy can be precise while unaffected by the disturbance position. Thus, the entire dynamic compliance control accuracy won't be affected by inner loop control accuracy. However, some real factors do affect the force control accuracy under the real conditions, such as the natural nonlinear characteristic of hydraulic system, the time-varied parameter, the uncertainty of environment and the load characteristic of hydraulic system. Especially the dynamic change of load characteristic will lead to a dynamic effect on the force control accuracy. It means that the HIVC force control inner loop itself possesses certain dynamic compliance which is not infinite. For the existence of certain compliance in the HIVC force control system, the accuracy of HIVC force control inner loop is decreased. More than that, the entire compliance control accuracy of the legged robot is also affected. Thus, it is necessary to figure out what dynamic compliance the HIVC force control system has and apply the dynamic compliance compensation control, which can make the self-dynamic-compliance of system tend to be the ideal condition further more. Then the control accuracy of force control inner loop can be increased effectively. Also, together with the impedance control outer loop, the force control inner loop can generate a combined effect on system and increase entire compliance control accuracy of system. So the entire motion performance of legged robot is improved.

In recent years, experts from many countries have conducted lots of researches on high accuracy and high robustness of force control system, not limited to the hydraulic force system. Part of those researches are listed as follows: Endo *et al.* [12] researched a simple boundary feedback controller that consists of the bending moment at the root of the flexible arm and its time derivative to solve the force control problem for a constrained one-link flexible arm. Yao *et al.* [13] researched a discontinuous projection-based nonlinear adaptive robust back-stepping force controller to improve the hydraulic load simulator force control robust performance. Wang *et al.* [14] researched an internal model controller including flow compensator, velocity compensator, internal model controller, which can improve the dynamic performance of force control system. Cao *et al.* [15] researched an adaptive finite-time motion/force control strategy using a new fast terminal sliding mode. Sariyildiz *et al.* [16] researched the robustness and stability of disturbance observer(DOb)-based explicit force control systems.

In those researches mentioned above, not limited to the cited ones, researchers analyzed the performance of force control system and optimized s force control performance, such as the accuracy, the dynamic characteristic, the ability of disturbance rejection and so on. All those measures brought better effectiveness to the system. However, some control methods adopted in those researches applied advanced control algorithms, which are complex and lack of engineering practicability. Besides, it is necessary to point out that the composition of self-dynamic-compliance of force control system wasn't proposed and studied in those researches. Yet in the authors' former researches, firstly, the method for system modeling, the performance analysis of position control and the sensitivity characteristics of system parameters were proposed and studied aimed at the HIVC position control system [17, 18]. Secondly, for the HIVC force control system, authors proposed the method for system modeling and researched the robustness control of force control system under the condition of variable load stiffness and damping [19]. The results from former researches lay foundation for research on dynamic compliance of force control system and compensation control in this paper. Combined with the analysis mentioned above and issues to be improved, the novelty and organization in this paper are listed as follows: firstly, the nonlinear mathematical model of HIVC force control system is introduced and the ideal dynamic compliance of force control system is discussed. Then the paper comes up with the experiment of force control system dynamic compliance under real conditions. Secondly, based on the mathematical model of HIVC force control system, this paper puts forward the dynamic compliance series composition theory as well as the dynamic compliance analysis of HIVC force control system. Thirdly, aimed at each part of dynamic compliance of HIVC force control system, the compound compensation control method of dynamic compliance with multiple series branches is designed and the series composition of system dynamic compliance is rearranged in the paper, which can enhance the dynamic compliance of HIVC force control system effectively. This is our main contribution. Finally, the availability of control method proposed in the paper is

proved by conducting experiment on the HIVC performance test platform. It provides the entire compliance control with the compliance compensation control strategy of force control inner loop.

2. Sampling system

2.1 Introduction of HIVC

2.1.1 Mathematical model

The HIVC is a highly integrated system of servo valve-controlled symmetrical cylinder, which is the hydraulic drive legged robot joint drive. It is shown in Fig. 1, including the quadruped robot prototype, the single leg hydraulic drive system and the HIVC.

The paper puts emphasis on the dynamic compliance of force control system and its compensation control method. The force closed-loop control transfer block diagram of HIVC should be built in advance, which is shown in Fig. 2 [19].

In Fig. 2, ω is natural frequency of servo valve, ζ is damping ratio of servo valve, $K_d = C_d W\sqrt{2/\rho}$ (K_d is defined as conversion coefficient in this paper), C_d is orifice flow coefficient of spool valve, W is area gradient of spool valve, ρ is density of hydraulic oil, p_s is system supply oil pressure, p_1 is left cavity pressure of servo cylinder, p_2 is right cavity pressure of servo cylinder, p_0 is system return oil pressure, C_{ip} is internal leakage coefficient of servo cylinder, C_{ep} is external leakage coefficient of servo cylinder, A_p is effective piston area of servo cylinder, β_e is effective bulk modulus, m_t is conversion mass(including the piston, the displacement sensor, the force sensor, the connecting pipe and the oil in servo cylinder), F_r is input Force, K_F is force sensor gain, K_{PID} is PID controller gain including proportional gain K_P, integral gain K_I and differential gain K_D, $K_{\alpha xv}$ is servo valve gain, K is load stiffness, B_p is load damping, X_L is load position, X_v is servo valve spool displacement, X_p is servo cylinder piston displacement, V_{g1} is volume of input oil pipe, V_{g2} is volume of output oil pipe, F_f is friction, U_r is input voltage, U_g is controller output voltage, Q_1 is inlet oil flow, Q_2 is outlet oil flow.

(a) Single leg

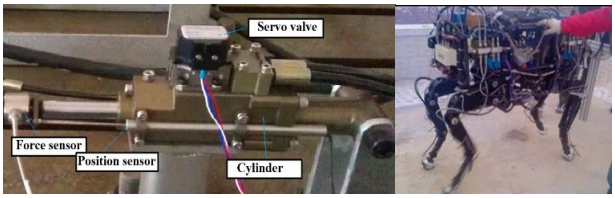

(b) Prototype (c) HIVC

Fig. 1. Hydraulic drive legged robot joint drive

2.1.2 Ideal dynamic compliance of HIVC force control system

The dynamic compliance is the ratio of system force variation to position variation. In terms of position control system, the dynamic compliance refers to ratio of system disturbance force to output position. When the system is under effect of disturbance force, the ratio getting larger indicates the output position variation getting smaller. So the dynamic compliance will get smaller, which means that the system tends to be the ideal position control system further more. While as for the force control system, the dynamic compliance turns to be ratio of system output force variation to disturbance position. When system is under disturbance position, the ratio getting smaller indicates the output force variation getting smaller. So the dynamic compliance will get larger, which means that the system tends to be the ideal force control system further more. In this section, the HIVC force control system is taken as the research object. The transfer block diagram simplified from Fig. 2 is shown in Fig. 3. Then it begins with the system dynamic compliance under the ideal condition.

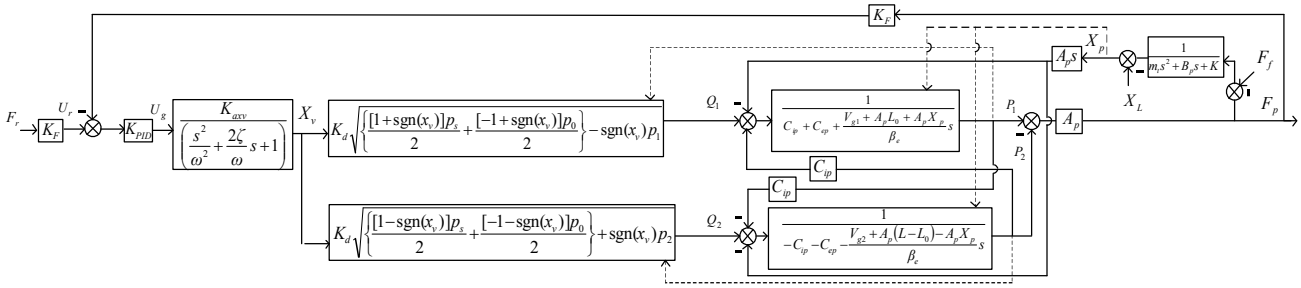

Fig. 2. Force closed-loop control transfer block diagram of HIVC

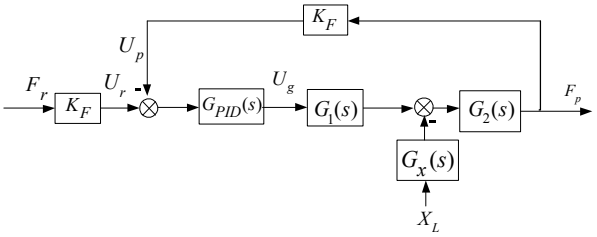

Fig. 3. Simplified transfer block diagram

In the diagram above, $G_x(s)$ is the transfer function which indicates that the disturbance position acts on system. Then $G_1(s)$ and $G_2(s)$ indicates the natural transfer functions of system respectively. All those three functions can be worked out according to the HIVC force control system transfer block diagram shown in Fig. 2. Due to the limited space, the solution process is not listed.

Therefore, the self-dynamic-compliance of HIVC force control system can be expressed as follows:

$$Z_{sf} = \frac{F_p}{X_L} \tag{1}$$

When the disturbance X_L acts on the system, there exists output force error. Assuming that the system is under ideal condition. In other words, the system response is fast enough and there is no leakage and friction in the system as well as the oil can't be compressed and so on. Thus, the force error can be completely compensated by system closed loop, which means that at any time: $U_p - U_r = 0$. Then in Eq. (1), $F_p = 0$. So, it shows that the output force of force control system isn't affected by disturbance position X_L, i.e. the system self-dynamic-compliance is infinite.

2.2 Experiment

2.2.1 Performance test platform

The schematic of HIVC performance test platform is shown in Fig. 4. The right part is a HIVC adopted force closed-loop control containing a small servo valve, servo cylinder, position sensor and force sensor, which is called the tested system. The left part is another HIVC adopted position closed-loop control containing the same type servo valve, servo cylinder, which is called the disturbance position simulation system. Two parts' cylinder rods are jointed rigidly by thread of force sensor. The photo of HIVC performance test platform is shown in Fig. 5.

The simulation model based on Fig. 2 are built by MATLAB/Simulink software. The parameters of the simulation models including amplifier, force sensor and servo valve are obtained from product book. The natural parameters of servo valve in the model are obtained from the fitted time domain and frequency domain characteristic curves according to the servo valve's product book.

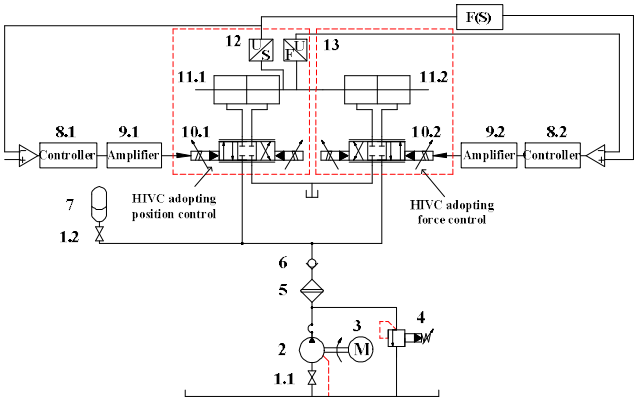

Fig. 4. The schematic of HIVC performance test platform

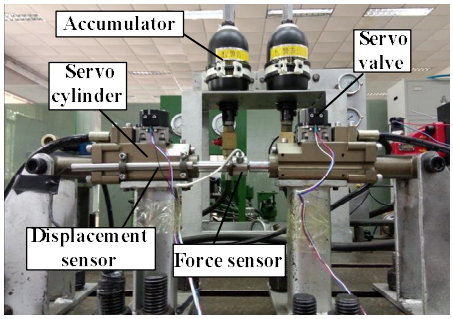

Fig. 5. The photo of HIVC performance test platform

Table 1. Parameters and initial value

Parameters	Initial value	unit
ω	628	rad/s
ζ	0.77	
K_{axv}	0.00045	m/v
A_p	3.368×10^{-4}	m^2
L	0.05	M
L_0	0.025	m
p_s	1×10^{7}	Pa
p_0	0.5×10^{6}	Pa
C_{ip}	2.38×10^{-13}	$m^3/(s\cdot Pa)$
β_e	8×10^{8}	Pa
K_d	1.248×10^{-4}	M^2/s
K_F	7.7×10^{-4}	V/N

Moreover, the structure parameters including effective piston area of servo cylinder, total piston stroke of servo cylinder and the volume of oil pipe are according to the factory data of the cylinder. The working parameters, including system supply oil pressure, system return oil pressure and sensor gain, are taken from the experiment test, while other parameters are selected through engineering experience. Therefore, the force control system simulation model parameters and initial value of HIVC are listed in Table 1.

2.2.2 Experiment

In the authors' former research [17-19], the disturbance

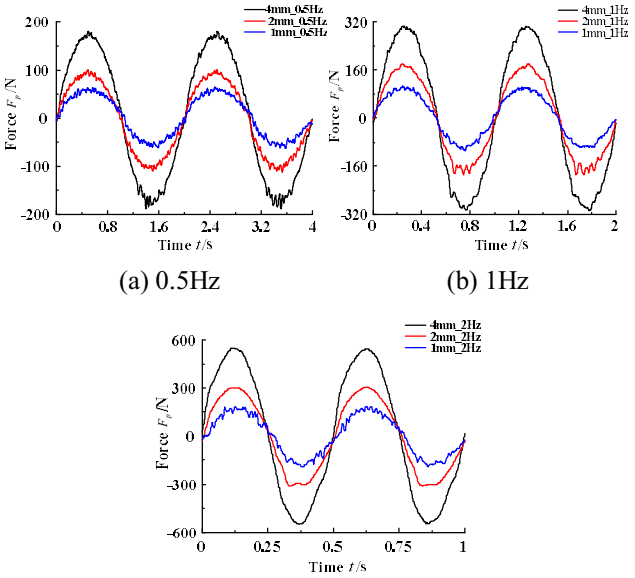

(a) 0.5Hz (b) 1Hz

(c) 2Hz

Fig. 6. Experimental curves under sinusoidal disturbance position

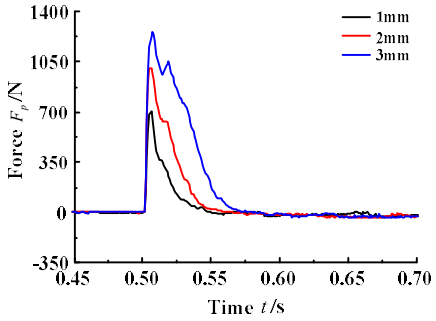

Fig. 7. Experimental curves under step disturbance position

position simulation effect of HIVC performance test platform as well as its force control performance was tested experimentally. The test result from former research proved the excellent control performance of the test platform, which is not listed in this paper. Whether the self-dynamic-compliance of HIVC force control system is ideal under the ideal condition will be tested in this section. Therefore, the sinusoidal disturbance position and the step disturbance position are applied to the HIVC force control system.

The initial position of force control system is set at the middle position and its value is 25mm. The amplitude of different sinusoidal disturbance position is 1mm, 2mm and 4mm in correspondence with the frequency of 0.5HZ, 1HZ and 2HZ respectively. Then the experimental curves are shown in Fig. 6.

When the system is under different disturbance position, the impact force acts on system. In order to test the impact force, the values of step disturbance position are set as 1mm, 2mm and 3mm. Then the experimental curves are shown in Fig. 7.

In Fig. 7, when the time is 0.5s, introducing the step disturbance position to system can generate a larger instant impact force on system. As the value of disturbance position gets increased, the instant force impact gets larger and it takes more time for the system return to the steady state. For example, when the value of step disturbance position is 1mm, the impact force is around 700N and it takes about 50ms for system to return to the steady state. While when the value of step disturbance position is 3mm, the impact force is around 1200N and it takes about 80ms for system to return to the steady state. The two groups of values above also indicate the HIVC force control system is not the ideal force control system. In other words, the system self-dynamic-compliance isn't infinite and it changes dynamically as the disturbance position changes.

In the following paper, the self-dynamic-compliance of force control system will be analyzed at length, also the compensation control strategy is put forward aimed at each part of dynamic compliance. All the researches are aimed at making the HIVC force control system tend to the ideal system when the disturbance position exists, i.e. the system can obtain rather large dynamic compliance.

3. Dynamic Compliance of HIVC Force Control System

3.1 Research value of dynamic compliance research

The dynamic compliance control method belonging to outer loop control method based on system inner loop control is widely researched in the robotic research domain. The system inner loop is mostly regarded as the ideal system in these researches. For the ability of quick response, the force closed loop control becomes the common method of inner loop control nowadays. In order to realize the precise force control in force control system, it is necessary to make the output force be in accordance with the input force all the time, which shows that the force control system should have infinite dynamic compliance, i.e. the output force is not affected by the disturbance position. However, some natural factors of the hydraulic system itself, such as the time-varied parameters, the strong coupling, the disturbance and the uncertainty of environment, make the hydraulic force control inner loop can't be regarded as the ideal system under real working conditions, which indicates that the self-dynamic-compliance of force control system is not infinite.

In this section, it begins with the analysis of dynamic compliance mechanism for HIVC force control system and then goes on with the compensation control method.

3.2 Dynamic compliance mechanism analysis

According to the experiment research shown in Section 2.2. (2), the HIVC force control system is affected by

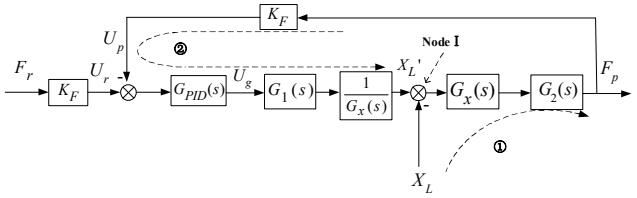

Fig.8. The HIVC force control system block diagram

multiple factors, such as the system response time, the oil compressibility, the leakage, the friction, the load characteristic and so on. Therefore, the system self-dynamic-compliance Z_{sf} can't be infinite.

In order to research the dynamic compliance of the HIVC force control system, it is necessary to analyze the system control block diagram in advance. The HIVC force control system block diagram transformed from Fig3. is shown in Fig. 8.

In Fig. 8, it is assumed that there is no force error between the input force and the output force in the HIVC force control system, which means that the error value of the voltage signal from input is zero, i.e. $U_P - U_r = 0$. Thus, the disturbance position X_L only affects the output force F_P along the way ①. Under that condition, a high order dynamic compliance Z_{sp}^1 in the system can be expressed as follows:

$$Z_{sf}^1 = \frac{F_P}{X_L} = -G_x(s)G_2(s) = \frac{\frac{m_t(V_1+V_2)A_p^2}{\beta_e}s^3 + \frac{V_1+V_2}{\beta_e}B_pA_p^2s^2 + \frac{V_1+V_2}{\beta_e}KA_p^2s + 2KC_{ep}A_p^2s}{\frac{m_tV_1V_2}{\beta_e^2}s^3 + \left[\frac{m_tC_{ip}(V_1+V_2)}{\beta_e} + B_p\frac{V_1V_2}{\beta_e^2}\right]s^2 + \left[\frac{V_1+V_2}{\beta_e}A_p^2 + \frac{B_pC_{ip}(V_1+V_2)}{\beta_e} + \frac{KV_1V_2}{\beta_e^2}\right]s + \frac{KC_{ip}(V_1+V_2)}{\beta_e}} \quad (2)$$

where

$$V_1 = V_{g1} + A_pL_0 + A_px_p \quad (3)$$

And,

$$V_2 = V_{g2} + A_pL_0 - A_px_p \quad (4)$$

In the Eq. 2), Z_{sf}^1 is referred to as the natural dynamic compliance of HIVC force control system. Both the numerator and the denominator of Z_{sf}^1 contain high order dynamic links. In other words, as the disturbance position X_L changes dynamically, the system output force F_p will be dynamic effect.

However, the dynamic compliance of force control

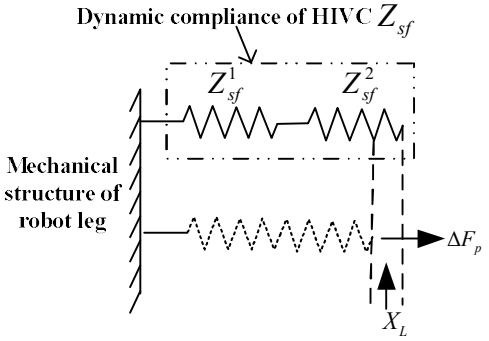

Fig. 9. Dynamic compliance schematic of HIVC force control system

system from Eq. (2) is obtained when the error value of the voltage signal from input is zero, i.e. $U_P - U_r = 0$. While under the real condition, this error value cannot be zero in real time during the response process. As can be seen in Fig. 8, due to this error value produced by force control system, the X_L' at Node I s produced to reduce the effect produced by disturbance position X_L. Under this condition, the other high order dynamic compliance Z_{sp}^2 can be obtained along the way ② in the force control system block diagram, which is expressed as follows:

$$Z_{sf}^2 = \frac{F_P}{X_L'} = -\frac{G_x(s)}{K_FG_{PID}(s)G_1(s)} = \frac{a_1s^6 + a_2s^5 + a_3s^4 + a_4s^3 + a_5s^2}{a_7s^3 + a_8s^2 + a_9s + a_{10}} \quad (5)$$

Due to limited space, the coefficients of all items are listed in the Appendix.

In the equation above, Z_{sf}^2 is referred to as the equivalent dynamic compliance generated by system closed loop control, which has an opposite direction. For the F_r is input signal unrelated to disturbance position, it can be seen that both Z_{sf}^1 and Z_{sf}^2 act on the output force F_P at the same time, i.e. the output force variation caused by those two dynamic compliances affects each other and corresponds to the same output force F_P. Therefore, those two dynamic compliances have a series relationship in the control system. The schematic is shown in Fig. 9, where the spring represents the dynamic compliance.

As can be seen in Fig. 9, the HIVC force control system is a series system made up by two dynamic compliances. When affected by disturbance position X_L, those two dynamic compliances generate same force error which is expressed as follows:

$$\Delta F_p = Z_{sf} \cdot X_L \quad (6)$$

Where the inner loop dynamic compliance Z_{sf} can be expressed as follows:

$$\frac{1}{Z_{sf}} = \frac{1}{Z_{sf}^1} + \frac{1}{Z_{sf}^2} \quad (7)$$

In Eq. (6) and Eq. (7), ΔF_p represents the system force error produced by Z_{sf}, and it affects the control accuracy of force control system. It is can be seen that the more the value of dynamic compliance tends to be zero, the larger the dynamic compliance is. Then the system force error gets smaller and the force control accuracy gets higher.

3.3 The compliance-enhanced control for HIVC force control system

It is discussed in Section 3.2 that the force error ΔF_p exits when disturbance position X_L acts on the system. And when the force error ΔF_p tends to be zero, the dynamic compliance of system gets infinite. Thus, in order to enhance the dynamic compliance of force control system at the most extent, which means ΔF_p tends to be zero under the condition of the outer loop disturbance position X_L, the compliance-enhanced controller is designed in this section.

As can be seen in Fig.8, if there is no force error in force control system, when the natural dynamic compliance Z_{sf}^1 tends to be zero so that it makes X_L has few effect on F_P, the error value of voltage signal from input will be zero, i.e. U_p-U_r=0. When U_p-U_r=0, the disturbance position X_L only affects the output force F_P along way ①, which means the dynamic compliance $Z_{sf} = Z_{sf}^1$. Therefore, making the controller be capable of compensating natural dynamic compliance Z_{sf}^1 completely and getting the value of Z_{sf}^1 to be zero become the primary idea of controller design, which can make the influence of X_L that acts on F_P tends to be zero. So the dynamic compliance Z_{sf}^2 along the way ② is invalid and the dynamic compliance of the force control system tends to be infinite.

According to the idea mentioned above, the feedforward compensation controller $G_{cf}^1(s)$ is designed to compensate system dynamic compliance and improve the system inner loop control accuracy. Then the compensation control schematic of HIVC force control system is shown in Fig. 10.

If
$$G_{cf}^1(s) = \frac{G_x(s)}{G_1(s)} \tag{8}$$

Ignore the effects of the initial force of HIVC to simplify the control compensation link, so V_1=V_2=$V_t/2$. Based on Fig. 8, the feedforward compensation controller $G_{cf}^1(s)$

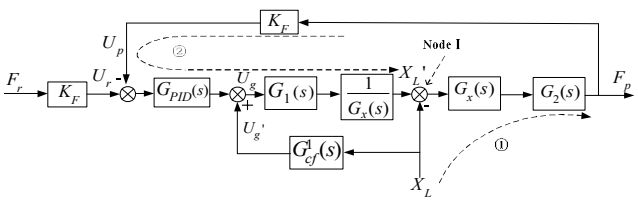

Fig. 10. The compensation schematic of the HIVC force control system

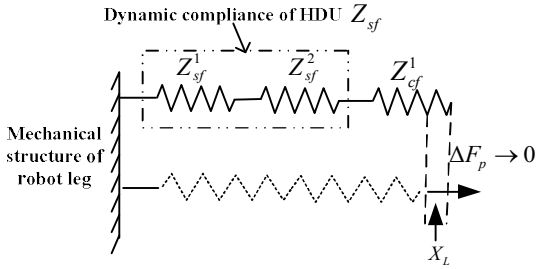

Fig. 11. Dynamic compliance schematic of the force control system

can be expressed as follows:

$$G_{cf}^1(s) = \frac{G_x(s)}{G_1(s)} = \frac{2A_p s\left(\frac{s^2}{\omega^2} + \frac{2\zeta}{\omega}s + 1\right)}{K_{axv}\left(K_1 + K_2\right)} = \frac{A_p s\left(\frac{s^2}{\omega^2} + \frac{2\zeta}{\omega}s + 1\right)}{K_{axv}K_d\sqrt{p_s - p_0 - \hat{p}_L}} \tag{9}$$

In Fig. 10, X_L' compensates X_L at Node I and it makes the system output F_P remain unchanged. In fact, that indicates the controller generate an equivalent controller dynamic compliance Z_{cf}^1 to compensate natural dynamic compliance Z_{sf}^1 in the system. Then the dynamic compliance schematic of HIVC force control system is shown in Fig. 11.

As can be seen in Fig.11, the equivalent controller dynamic compliance Z_{cf}^1 generates a dynamic compliance with the opposite direction to the dynamic compliance Z_{sf}^1.

However, high frequency noise exists in the test values generated by position sensor. In order to reduce the influence of noise by conducting effective signal filter, Butterworth filter method is adopted in the experiment. During the process of experiment, the signal collected by position sensor is transformed into the compensation voltage U_g' through the controller. Yet it is observed that the compensation voltage U_g' fluctuates drastically when the controller's second order differentiation links and higher order differentiation links is adopted, which reduces the control effect observably. So the optimization of $G_{cf}^1(s)$ aimed at higher order differentiation link should be applied and the Eq. (9) can be transformed into:

$$Q_L = K_d\sqrt{p_s - p_0 - \hat{p}_L}X_v \tag{12}$$

The equation above contains two state vectors $\hat{p}_L$ and x_v. It is expanded by first order Taylor formula:

$$\begin{aligned} Q_L &= K_d\sqrt{p_s - p_0 - \hat{p}_L}X_v - \frac{K_d X_v}{2\sqrt{p_s - p_0 - \hat{p}_L}}\hat{p}_L \\ &= K_q X_v - K_c\hat{p}_L \end{aligned} \tag{13}$$

It can be seen in the equation above, when the X_L increases, the load pressure $\hat{p}_L$ increases while the load

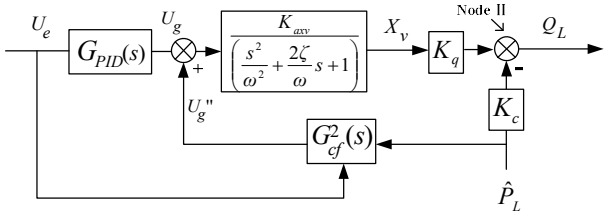

Fig. 12. Simplified compensation schematic of $G_{cf}^2(s)$

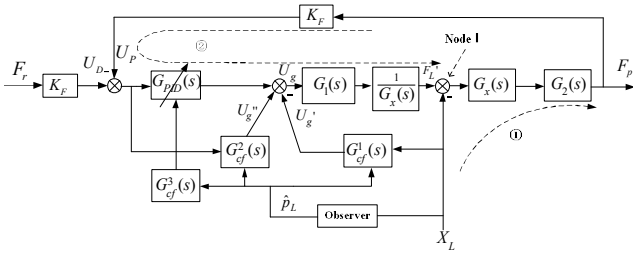

Fig. 13. Force control system compensation schematic

flow Q_L decreases, which reduces the rapidity of the compensation supplied by dynamic compliance Z_{sf}^2 for system.

The simplified control block diagram of input end voltage error to load flow is shown in Fig. 12.

When

$$G_{cf}^2(s)=\frac{K_c K_{PI} X_v}{K_q K_{axv}}\left(\frac{s^2}{\omega^2}+\frac{2\zeta}{\omega}s+1\right)=\frac{K_{adapt} K_{PI} U_e}{2(p_s-p_0-\hat{p}_L)} \quad (14)$$

In the equation above, K_{adapt} is the voltage compensation self-adaption coefficient. The setting of this coefficient is referred to the basic theory of adaptive interaction [20, 21]. Based on the equation above, the variation of load flow Q_L is reduced at node II in Fig. 12 by compensating at the servo value voltage input end. In fact, it is the feedforward compensation controller $G_{cf}^2(s)$ that generates equivalent controller dynamic compliance Z_{cf}^2 to compensate equivalent dynamic compliance Z_{sf}^2.

In order to improve the control robustness of controller $G_{cf}^1(s)$ and $G_{cf}^2(s)$ further, the parameter self-tuning PID controller $G_{cf}^3(s)$ is applied to adjust the system forward path gain online, which is designed in authors' former research [18, 19].

Then the compensation control schematic of HIVC force control system is shown in Fig. 13.

The dynamic compliance schematic of HIVC force control system is shown in Fig. 14.

Combined with the controller $G_{cf}^1(s)$, $G_{cf}^2(s)$ and $G_{cf}^3(s)$, the compound compliance-eliminated controller $G_{cf}(s)$ is worked out in this paper. That compound controller is designed to reduce the dynamic compliance value of HIVC force control system and make the dynamic compliance tend to be infinite. Among those three controllers, the controller $G_{cf}^1(s)$ acts on the first dynamic

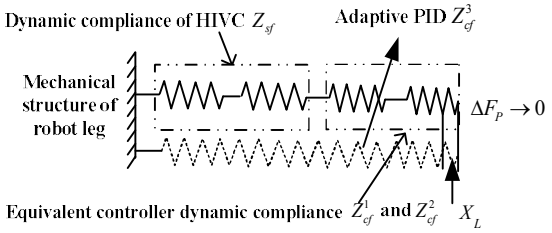

Fig. 14. Dynamic compliance of force control system

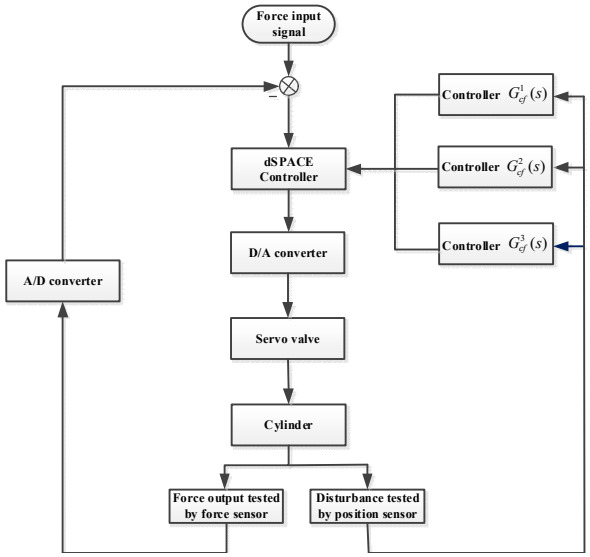

Fig. 15. Flowchart of control technique

compliance Z_{sf}^1 while the controller $G_{cf}^2(s)$ and $G_{cf}^3(s)$ act on the second dynamic compliance Z_{sf}^2 together.

3.4 Experimental result

3.4.1 Control schematic of the experiment

Used in the HIVC performance test platform, the flowchart of control technique and the process model is shown in Fig. 15, and the schematic of compliance-enhanced controller is shown in Fig. 16.

3.4.2 Experiment of sinusoidal response

Based on the schematic shown in Fig. 15, the effectiveness of the controllers designed in this paper can be verified in the experiment. Under the different working conditions mentioned in Section 2.2, the experimental curves are obtained and shown in Fig. 17. Each picture of Fig. 17 has four curves.

The enhancement ratios of dynamic compliance under different working conditions are shown quantitatively in Table 2. (the enhancement ratio of dynamic compliance under sinusoidal disturbance position = the eliminated output force error after control / the output force error before control; ① represents only adopting controller

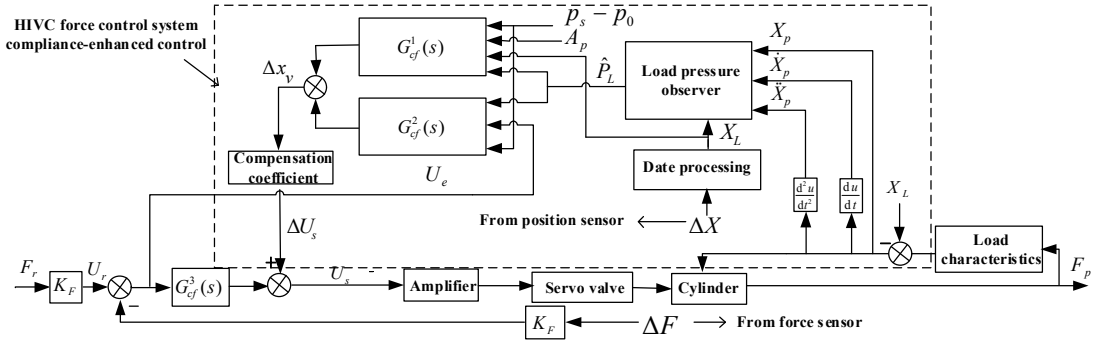

Fig. 16. Schematic of the experiment

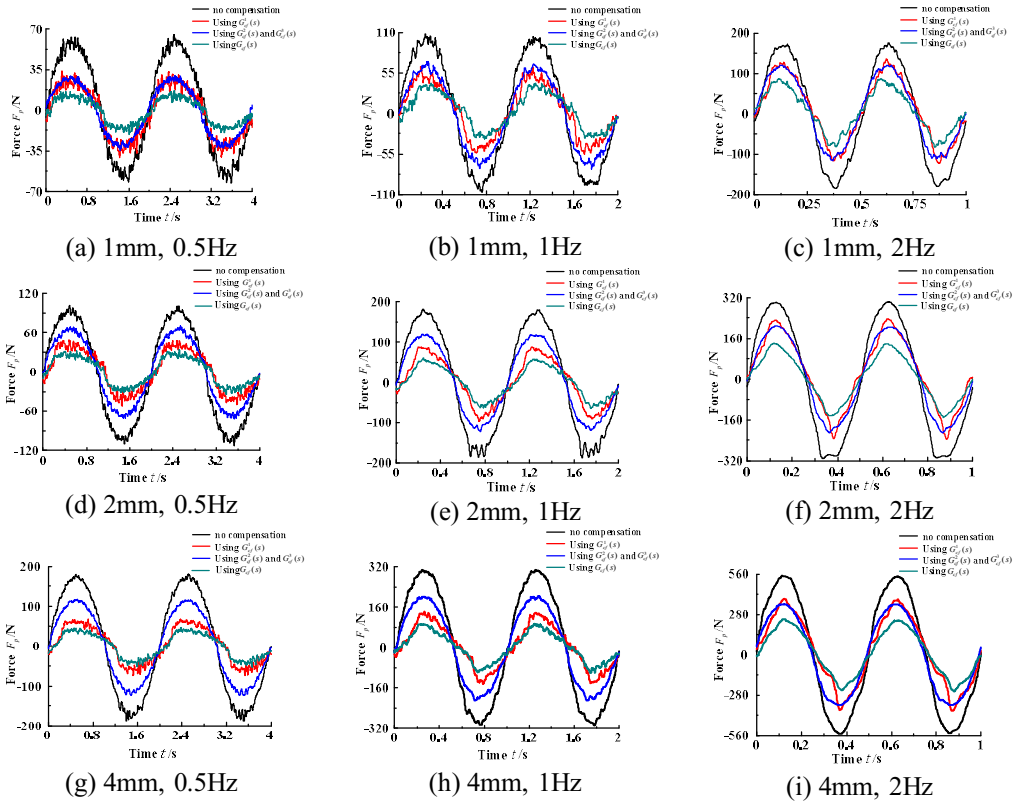

(a) 1mm, 0.5Hz (b) 1mm, 1Hz (c) 1mm, 2Hz

(d) 2mm, 0.5Hz (e) 2mm, 1Hz (f) 2mm, 2Hz

(g) 4mm, 0.5Hz (h) 4mm, 1Hz (i) 4mm, 2Hz

Fig. 17. Experimental curves under sinusoidal disturbance

Table 2. Mean and peak enhancement ratio under sinusoidal disturbance position(Accurate to one decimal places %)

X_L	1mm						2mm						4mm					
	Mean			Peak			Mean			Peak			Mean			Peak		
	①	②	③	①	②	③		②	③	①	②	③	①	②	③	①	②	③
0.5Hz	48.3	49.4	74.4	58.3	56.7	78.3	56.4	30.3	70.7	57.9	31.3	72.9	63.8	33.4	75.7	65.3	34.1	78.0
1Hz	49.9	37.4	63.3	51	38.2	64.7	49.5	32.0	67.6	51.4	33.1	69.7	55.6	33.0	68.1	57.3	34.1	70.2
2Hz	27.2	28.2	49.8	28.6	29.8	52.4	28.3	28.5	51.0	29.1	30.4	53.4	29.2	35.0	53.7	30.1	36.1	55.4

$G_{cf}^1(s)$; ② represents only adopting controller $G_{cf}^2(s)$ and $G_{cf}^3(s)$; ③ represents adopting controller $G_{cf}(s)$)

As can be seen in Table 2, under different working conditions, the dynamic compliance of force control system gets enhanced at some extent after applying the controller $G_{cf}^1(s)$ to the system alone. Especially when the frequency of disturbance position is lower or the amplitude of disturbance position is larger, the system can receive a better control effect.

After applying the controller $G_{cf}^2(s)$ and $G_{cf}^3(s)$ to the system alone, the dynamic compliance of force control system also gets enhanced at some extent. But under

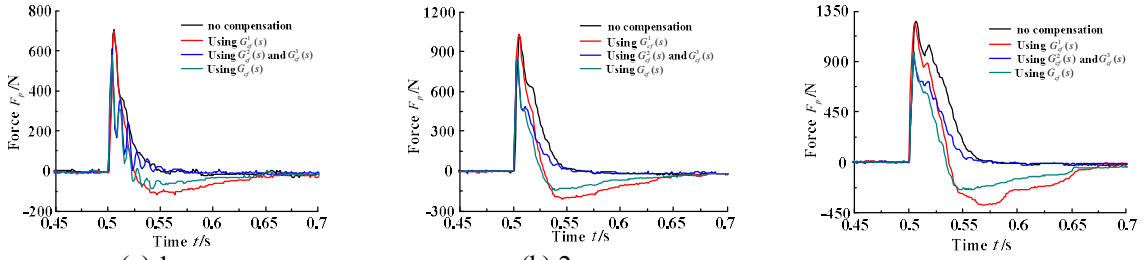

(a) 1mm (b) 2mm (c) 4mm

Fig. 18. Experimental curves under the step disturbance

Table 3. Peak enhancement ratio of dynamic compliance under the step disturbance position (Accurate to one decimal places %)

Step	Control number	Peak
1mm	①	0.9
	②	13.5
	③	18.0
2mm	①	-0.5
	②	17.7
	③	18.3
4mm	①	1.0
	②	22.2
	③	21.7

different working conditions, the system receives different control effect compared with the condition where the controller $G_{cf}^1(s)$ is applied to the system alone. Especially when the frequency of disturbance position is lower or the amplitude of disturbance position is smaller, the system can receive a better control effect.

While after applying the compound controller $G_{cf}(s)$ made up by controller $G_{cf}^1(s)$, $G_{cf}^2(s)$ and $G_{cf}^3(s)$ to the system, the system dynamic compliance gets enhanced further more than the condition where any controller is applied to the system alone.

3.4.3 Experiment of step response

The experiment is conducted under the same working conditions as those from Section 2.2. The experimental curves are shown in Fig.18. Each picture of Fig.18 has four curves. And those curves are obtained under different experimental conditions, which are condition without compensation, condition with controller $G_{cf}^1(s)$ used, condition with controller $G_{cf}^2(s)$ and $G_{cf}^3(s)$ used and condition with compound controller $G_{cf}(s)$ used.

The enhancement ratios of dynamic compliance under different working conditions are shown quantitatively in Table 3.

As can be seen in Table 3, the peak impact force is barely eliminated after applying the controller $G_{cf}^1(s)$ to system alone. That phenomenon can be explained as follows: For the first order differential items of the numerator exist in Eq. (11) and the acceleration of step response tends to infinite, the compensation signal generated by controller $G_{cf}^1(s)$ tends to be zero. But in the experiment, the controller can still generate slight compensation signal. As the real step disturbance position is simulated by the position control system, it needs certain time for hydraulic cylinder to move to the step position. Actually, that move process is a short dynamic process. Therefore, the controller $G_{cf}^1(s)$ provides few control effect. However, after applying controller $G_{cf}^2(s)$ and $G_{cf}^3(s)$ to the system alone, the compensation effect can be obtained for eliminating the peak impact force. Besides, the system can obtain different compensation effect under different step disturbance position.

In Fig. 18, under different disturbance position, the controller $G_{cf}^1(s)$ barely eliminates the peak impact force and it generates opposite impact force. The peaks of those opposite impact force are about 118N, 213N and 384N. That brings negative control effect to the system. While the controller $G_{cf}^2(s)$ and $G_{cf}^3(s)$ can supply compensation to the peak enhancement ratio. As the step disturbance position get increased, the control effect gets better and the opposite impact force is hardly generated. In conclusion, when the disturbance position signal changes instantaneously (such as the step response) and the system doesn't obtain the best control effect of dynamic compliance, the controller $G_{cf}^1(s)$ should not be turned on. While when the disturbance position signal changes dynamically, the compound controller $G_{cf}(s)$ should be turned on and it can bring excellent control effect to the system.

4. Conclusion

From the research and work mentioned above, the conclusion is listed as follows:

Firstly, the self-dynamic-compliance of HIVC force control system is larger. That dynamic compliance contains two parts. The first part is the natural dynamic compliance Z_{sf}^1, which is caused by the system natural link. The other part is the equivalent dynamic compliance Z_{sf}^2, which is generated equivalently by system force closed loop control. Those two compliances with the series relationship both act on the system during the process of system force closed loop control.

Secondly, aimed at the dynamic compliance Z_{sf}^1, the

compliance-enhanced controller $G_{cf}^{1}(s)$ is designed in this paper. That controller can generate an equivalent controller dynamic compliance Z_{cf}^{1} whose direction is opposite to the direction of Z_{sf}^{1}. Due to the series relationship of Z_{sf}^{1} and Z_{cf}^{1}, the entire system dynamic compliance reflected by Z_{sf}^{1} and Z_{cf}^{1} in series can be infinite theoretically.

Thirdly, aimed at the dynamic compliance Z_{sf}^{2}, the other compliance-enhanced controller $G_{cf}^{2}(s)$ is designed in this paper. Combined with the basic theory of adaptive interaction, that controller can supply the feedforward compensation to the system at the voltage input end of servo value. And it can compensate the reduction of load flow Q_L caused by the load position. Therefore, an equivalent controller dynamic compliance Z_{cf}^{2} is generated in the system, whose direction is the same as the direction of Z_{sf}^{2}. Due to the series relationship of Z_{cf}^{2} and Z_{sf}^{2}, the entire system dynamic compliance reflected by Z_{sf}^{1} and Z_{cf}^{1} in series also gets enhanced. Besides, based on the conditions mentioned above, the parameter self-tuning PID controller $G_{cf}^{3}(s)$ is applied to the system, which can increase the control robustness of controller $G_{cf}^{1}(s)$ and $G_{cf}^{2}(s)$.

Through the research and work in this paper, aimed at different working conditions, the compound compliance-enhanced controller $G_{cf}(s)$ is designed by combining three controllers together, which are $G_{cf}^{1}(s)$, $G_{cf}^{2}(s)$ and $G_{cf}^{3}(s)$. That compound controller enhances the self-dynamic-compliance of HIVC force control system greatly. Thus, the research result of this paper can be adopted as the hydraulic system inner loop compliance compensation control method for the entire motion control of the hydraulic drive robot and increase the accuracy and the robustness of the robotic outer loop compliance control.

Acknowledgements

This work was supported by National Natural Science Foundation of China (Grant no. 51605417), Key Project of Hebei Province Natural Science Foundation (Grant no. E2016203264)

References

[1] Gao, J., H. Li, H. Liu, Liu Y, et al, "The modeling and controlling of electrohydraulic actuator for quadruped robot based on fuzzy Proportion Integration Differentiation controller," *Journal of Mechanical Engineering and Science*, vol. 228, no. 14, pp. 2557-2568, 2014.

[2] Irawan, A. and K. Nonami, "Optimal impedance control based on body inertia for a hydraulically driven hexapod robot walking on uneven and extremely soft terrain," *Journal of Field Robotics*, vol. 28, no. 5, pp. 690-713, 2011.

[3] Polkovnikov, V. A., "Synthesis of the main parameters of servo actuators of hydraulic control surface drives of aircraft with a pump-controlled speed regulation," *Journal of Computer and Systems Sciences International*, vol. 41, no. 4, pp. 617-627, 2002.

[4] Sangpet, T; Kuntanapreeda, S., "Force control of an electrohydraulic actuator using a fractional-order controller," *Asian Journal of Control*, vol. 15, no. 3, pp. 764-772, 2013.

[5] Kimura, H., Y. Fukuoka, and A. H. Cohen, "Adaptive dynamic walking of a quadruped robot on natural ground based on biological concepts," *International Journal of Robotics Research,* vol. 26, no. 5, pp. 475-490, 2007.

[6] Poulakakis, I., J. A. Smith, and M. Buehler, "Modeling and experiments of untethered quadrupedal running with a bounding gait: the Scout II robot," *International Journal of Robotics Research*, vol. 24, no. 4, pp. 239-256, 2005.

[7] Nichol, J. G., S. P. N. Singh, and K. J. Waldron, et al, "System design of a quadrupedal galloping machine," *International Journal of Robotics Research*, vol. 23, no. 10-11, pp. 1013-1027, 2004.

[8] Playter, R., M. Buehler, and M. R, "Bigdog," *Proc. of the Conf. SPIE*, San Jose, USA, 2006.

[9] Claudio, S., "HyQ-Design and Development of a Hydraulically Actuated Quadruped Robot," Dissertation*,* University of Genoa, 2010.

[10] Rong, X. W., Y. B. Li, B. Yi, and B. Li, "Design and simulation for a hydraulic actuated quadruped robot," *Journal of Mechanical Science and Technology*, vol. 26, no. 4, pp. 1171-1177, 2012.

[11] Claudio, S., B. Victor, B. Thiago, and F. Marco, et al, "Towards versatile legged robots through active impedance control," *International Journal of Robotics Research*, vol. 34, no. 7, pp. 1003-1020 (2015).

[12] Takahiro E., Matsuno F., and Kawasaki H., "Force control and exponential stabilisation of one-link flexible arm," *International Journal of Control*, vol. 87, no. 9, pp. 1784-1807, 2014.

[13] Yao J. Y., Z. X. Jiao, and B. Yao, "Nonlinear adaptive robust backstepping force control of hydraulic load simulator: Theory and experiments," *Journal of Mechanical Science and Technology*, vol. 28, no. 4, pp. 1499-1507, 2014.

[14] Wang, Z. W., R. Z. Duan, G. T. Sun, and M. S. Chi, "Hydraulic quadruped robot joint force control based on double internal model controller," *International Journal of Control and Automation*, vol. 9, no. 1, pp. 241-250, 2016.

[15] Cao, Q. l., S. R. Li, D. Y. Zhao, "Adaptive motion/force control of constrained manipulators using a new fast terminal sliding mode," *International Journal of Computer Applications in Technology*, vol. 49, no. 2, pp. 150-156, 2014.

[16] Sariyildiz E., K. Ohnishi, "On the explicit robust force

control via disturbance observer," *IEEE Transactions on Industrial Electronics*, vol. 62, no. 3, pp. 1581-1589, 2015.
[17] Kong X. D., K. X. Ba, B. Yu, and Y. Cao, et al, "Trajectory sensitivity analysis of first order and second order on position control system of highly integrated valve-controlled cylinder," *Journal of Mechanical Science and Technology*, vol. 29, no. 10, pp. 4445-4464, 2015.
[18] K. X. Ba., B. Yu, Z. J. Gao and W. F. Li, et al. Parameters Sensitivity Analysis of Position-Based Impedance Control for Bionic Legged Robots' HDU, Applied Science, vol. 7, pp. 1035, 2017.
[19] Kong X. D., K. X. Ba, B. Yu, et al. "Research on the force control compensation method with variable load stiffness and damping of the hydraulic drive unit force control system," *Chinese Journal of Mechanical Engineering* (*English Edition*), vol. 29, no. 3, pp. 454-464, 2016.
[20] Lin F., R. D. Brandt, G. Saikalis, "Self-tuning of PID controllers by adaptive interaction," *Proc. of the American Control Conference*," vol. 5, pp. 3676-3681, 2000.
[21] Hazrin N., I. Elamcazuthi, "Closed-loop Force Control for Haptic Simulation Sensory Mode Interaction," *2009 Conference on Innovative Technologies in Intelligent Systems and Industrial Applications* (*CITISIA 2009*), pp. 96-100, 2009.

Appendix

Eq. (3) shown in section 3.2 is

$$Z_{sf}^2 = \frac{F_P}{X_L^{'}} = -\frac{G_x(s)}{K_F G_{PID}(s) G_1(s)} = \frac{a_1 s^6 + a_2 s^5 + a_3 s^4 + a_4 s^3 + a_5 s^2}{a_7 s^3 + a_8 s^2 + a_9 s + a_{10}}$$

where

$$a_1 = \frac{m_t (V_1 + V_2) A_p^2}{\beta_e \omega^2},$$

$$a_2 = \frac{2\zeta m_t (V_1 + V_2) A_p^2}{\beta_e \omega} + \frac{(V_1 + V_2) B_p A_p^2}{\beta_e \omega^2},$$

$$a_3 = \frac{m_t (V_1 + V_2) A_p^2}{\beta_e} + \frac{2\zeta}{\omega} \frac{V_1 + V_2}{\beta_e} B_p A_p^2 + \frac{K (V_1 + V_2) A_p^2}{\beta_e \omega^2},$$

$$a_4 = \frac{V_1 + V_2}{\beta_e} B_p A_p^2 + \frac{2\zeta (V_1 + V_2)}{\beta_e \omega} K A_p^2,$$

$$a_5 = \frac{V_1 + V_2}{\beta_e} K A_p^2 \quad a_7 = \frac{K_{axv} K_F K_p m_t A_p (K_1 V_2 + K_2 V_1)}{\beta_e},$$

$$a_8 = K_{axv} K_F \left[\frac{K_I m_t A_p (K_1 V_2 + K_2 V_1)}{\beta_e} + \frac{K_p B_p A_p (K_1 V_2 + K_2 V_1)}{\beta_e} \right],$$

$$a_9 = K_{axv} K_F \left[\frac{K_p K A_p (K_1 V_2 + K_2 V_1)}{\beta_e} + \frac{K_I B_p A_p (K_1 V_2 + K_2 V_1)}{\beta_e} \right],$$

$$a_{10} = \frac{K_{axv} K_F K_I K A_p (K_1 V_2 + K_2 V_1)}{\beta_e}$$

Xiang-Dong Kong He is a professor at Yanshan University, China. He serves as the chairman of Fluid Transmission and Control Society which is a branch of Chinese Mechanical Engineering Society (CMES). His main research interests include electro-hydraulic servo control system, heavy machinery fluid transmission and control and robot design and control.

Kai-Xian Ba He received his M.S. degree from Yanshan University, China, in 2014. His main research interests include electro-hydraulic servo control system and robot design and control.

Bin Yu He received his Ph.D. degree from Yanshan University, China, in 2015. His main research interests include heavy machinery fluid transmission and control and robot design and control.

Wen-Feng Li He is a Master student in Yanshan University, China. His main research interests include electro-hydraulic servo control system and robot design and control.

Dong-kun Wang He is a Master student in Yanshan University, China. His main research interests include electro-hydraulic servo control system and robot design and control.

Ya-liang Liu He is a Master student in Yanshan University, China. His main research interests include electro-hydraulic servo control system and robot design and control.

Guo-liang Ma He is a Master student in Yanshan University, China. His main research interests include electro-hydraulic servo control system and robot design and control.